ISSN 1070-3284, Russian Journal of Coordination Chemistry, 2019, Vol. 45, No. 8, pp. 585–591. © Pleiades Publishing, Ltd., 2019.
Russian Text © The Author(s), 2019, published in Koordinatsionnaya Khimiya, 2019, Vol. 45, No. 8, pp. 497–503.

# The Nature of Conformational Polymorphism in the Crystals of $Ph_3Sb(O_2CCH_2–CH=CH_2)_2$

**G. K. Fukin[a], *, E. V. Baranov[a], A. V. Cherkasov[a], and R. V. Rumyantsev[a]**

[a] *Razuvaev Institute of Organometallic Chemistry, Russian Academy of Sciences, Nizhny Novgorod, 603137 Russia*

**e-mail: gera@iomc.ras.ru*

Received December 27, 2018; revised February 1, 2019; accepted March 14, 2019

**Abstract**—Crystallization of the $Ph_3Sb(O_2CCH_2–CH=CH_2)_2$ complex upon fast solvent (benzene) evaporation gives monoclinic crystals (**I**), whereas in the case of slow evaporation, triclinic crystals are formed (**II**). Also, monoclinic crystals are spontaneously transformed into triclinic crystals within 6 months. It was shown that the presence of voids near one carboxylate ligand in the monoclinic phase of $Ph_3Sb(O_2CCH_2–CH=CH_2)_2$ decreases the energy of intermolecular interactions and, as a consequence, leads to a conformational transition with a noticeable decrease in the crystal lattice energy. Thus, the presence of voids in the monoclinic phase crystal allows the formation of a thermodynamically more favorable conformation of the molecule in the crystal. Several structural models were determined for the $Ph_3Sb(O_2CCH_2–CH=CH_2)_2$ complex (CIF files no. 1887561 ($\mathbf{I}_{IAM}$), model of non-interacting atoms; 1887562 (**I**), multipole model; 1887563 ($\mathbf{II}_{IAM}$), model of non-interacting atoms; 1887564 (**II**), multipole model).

*Keywords:* triphenylantimony complex with vinylacetic acid, high-precision X-ray diffraction, conformational polymorphs, Bader's theory of atoms in molecules

**DOI:** 10.1134/S1070328419080025

## INTRODUCTION

Carboxylate complexes of triarylantimony exhibit antitumor activity [1–8], which is potentially important for the treatment of cancer. However, these drugs also have adverse effects, first of all, high toxicity. Therefore, most studies of Sb(V) carboxylate derivatives address the relationship between the chemical and pharmacological properties of these compounds with the goal to minimize adverse effects and increase the efficacy of drugs. Of wide practical interest are studies on the use of triarylantimony carboxylate complexes in the polymerization [9–11], cross-coupling reactions [12–14], and also in the design of photoresists for microelectronics [15]. Also, we found that during crystallization of the $Ph_3Sb(O_2CCH_2–CH=CH_2)_2$ complex (**I**), fast evaporation of the solvent (benzene) results in the formation of monoclinic crystals, whereas slow evaporation gives triclinic crystals. Monoclinic crystals are spontaneously transformed into triclinic crystals within six months.

The present study is devoted to the causes of spontaneous monoclinic to triclinic transition of $Ph_3Sb-O_2CCH_2–CH=CH_2)_2$ (**I**).

## EXPERIMENTAL

The triphenylantimony(V) vinylacetate complex **I** was prepared by a known procedure described in [16].

**High-precision X-ray diffraction** study of complex **I** and its conformational polymorph (**II**) was carried out at 100 K on Oxford Xcalibur (Eos detector) (for **I**) and Bruker D8 QUEST (CMOS detector) (for **II**) automated diffractometers (graphite monochromators, Mo$K_\alpha$ radiation, $\lambda$ = 0.71073 Å). The experimental sets of reflection intensities were integrated using CrysAlisPro [17] and SAINT [18] programs. The SCALE3 ABSPACK [19] and SADABS program packages [20] were used to apply absorption corrections. The structures were solved by the direct method and refined by full-matrix least-squares method on $F^2$ (SHELXTL) [21]. All non-hydrogen atoms were refined in the anisotropic approximation. Hydrogen atoms were placed into geometrically calculated positions and refined isotropically with the riding model.

The multipole refinement of complexes **I** and **II** was performed using the Hansen–Coppens model [22] and the MoPro program package [23]. In the high-precision X-ray diffraction, all hydrogen atoms were normalized prior to the multipole refinement to the ideal neutron diffraction-derived lengths [24]. The multipole expansion level was hexadecapole for the antimony atom, octapole for all non-hydrogen atoms, and dipole for hydrogen atoms. All bonded pairs of atoms satisfied the Hirshfeld test [25]. The topological analysis of the experimental $\rho(\mathbf{r})$ function was performed using the WINXPRO software package [26].

**Table 1.** Key crystallographic characteristics and high-precision X-ay diffraction parameters for the multipole refinement model of complexes **I** and **II**

| Parameter | Value | |
|---|---|---|
| | **I** | **II** |
| Molecular formulas | $C_{26}H_{25}O_4Sb$ | $C_{26}H_{25}O_4Sb$ |
| *M* | 523.216 | 523.216 |
| System | Monoclinic | Triclinic |
| Space group | $P2_1/c$ | $P\bar{1}$ |
| *a*, Å | 12.4174(2) | 8.1823(3) |
| *b*, Å | 22.1246(4) | 8.8194(3) |
| *c*, Å | 8.8020(2) | 17.9141(7) |
| α, deg | 90 | 77.880(1) |
| β, deg | 104.647(2) | 89.821(1) |
| γ, deg | 90 | 62.885(1) |
| *V*, Å$^3$ | 2339.59(8) | 1118.62(7) |
| *Z* | 4 | 2 |
| ρ(calcd.), g cm$^{-3}$ | 1.486 | 1.554 |
| μ, mm$^{-1}$ | 1.208 | 1.263 |
| *F*(000) | 1056 | 528 |
| Crystal size, mm | 0.45 × 0.35 × 0.20 | 0.46 × 0.18 × 0.16 |
| Range of θ, deg | 3.02–51.42 | 2.34–51.43 |
| Number of collected/unique reflections | 971802/25476 | 336077/28905 |
| $R_1/wR_2$ ($I > 2\sigma(I)$) | 0.0394/0.0314 | 0.0177/0.0144 |
| GOOF | 0.993 | 0.998 |
| Residual electron density, e Å$^{-3}$ | 0.320/–0.449 | 0.311/–0.856 |

The presence of a disordered allyl moiety in **II** induces some deviations from the standard multipole refinement scheme, in which the atomic coordinates and thermal and multipole parameters were refined successively. Here we split the molecule into two blocks, one containing atoms with 100 and 80% site occupancy and the other containing only atoms with 20% occupancy. The same parameters were first refined in one block (100% + 80% occupancy) and then in the other block (20% occupancy), and this was done for each parameter to be refined. In addition, because of disorder of the allyl moiety, we applied the WINXPRO program to separately analyze the electron density topologies of two different conformations of **II** (**IIa** and **IIb**). In this case, site occupancy for each disordered allyl moiety was equal to unity.

The key crystallographic characteristics and X-ray diffraction parameters for the multipole refinement model for complexes **I** and **II** are summarized in Table 1.

The structures were deposited in the Cambridge Crystallographic Data Centre (CCDC) (no. 1887561 ($\mathbf{I}_{IAM}$), model of non-interacting atoms; 1887562 (**I**), multipole model; 1887563 ($\mathbf{II}_{IAM}$), model of non-interacting atoms; 1887564 (**II**), multipole model; http://www.ccdc.cam.ac.uk/data_request/cif).

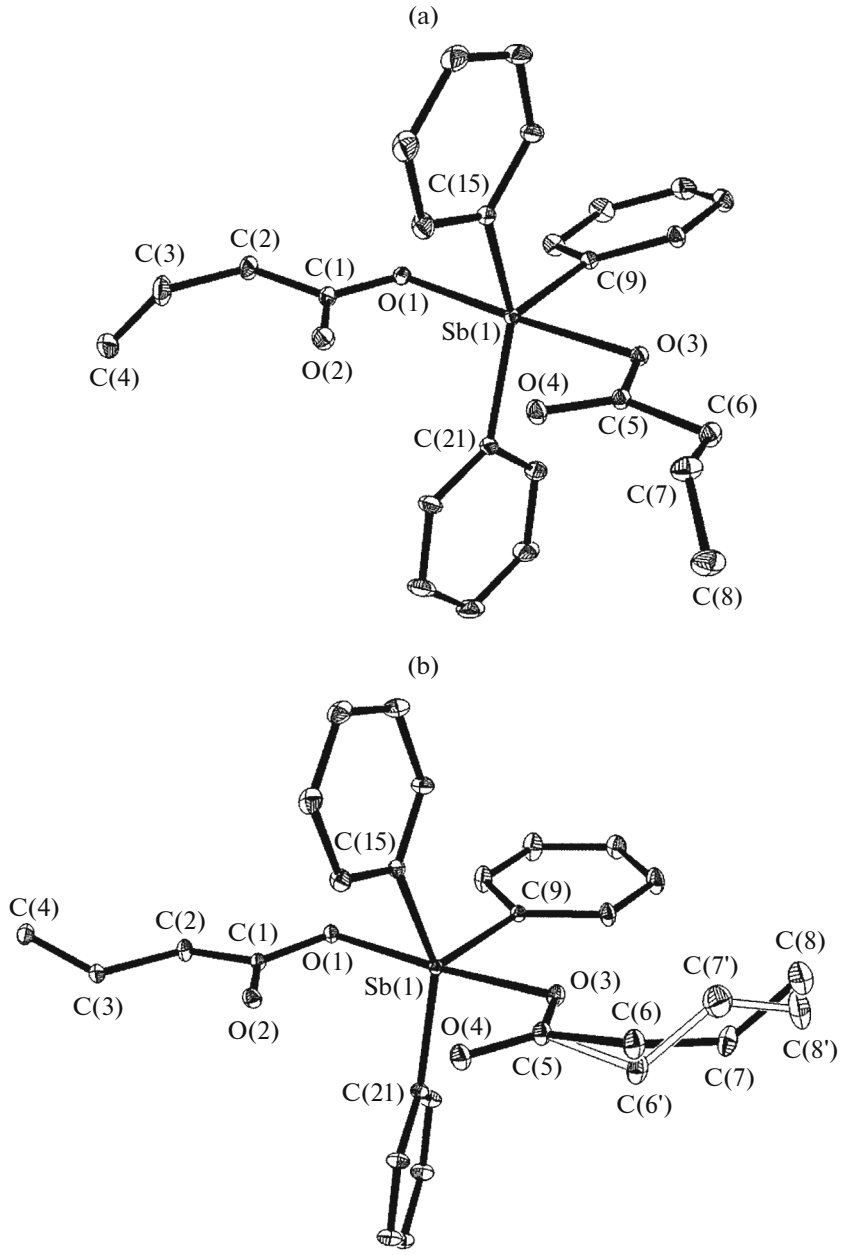


**Fig. 1.** Molecular structure of $Ph_3Sb(O_2CCH_2{-}CH{=}CH_2)_2$: (a) molecule of the monoclinic phase (**I**); (b) molecule of the triclinic phase (**II**). One carboxylate ligand in **II** is disordered over two sites with 80% occupancy (C(6)C(7)C(8) moiety, compound **IIa**) and 20% occupancy (C(6')C(7')C(8') moiety, compound **IIb**). The thermal ellipsoids are drawn at the 30% probability level. Hydrogen atoms are omitted for clarity.

## RESULTS AND DISCUSSION

In order to study the spontaneous phase transition of monoclinic crystals **I** to triclinic crystals **II**, their high-precision X-ray diffraction analysis was performed. The molecular structure of the complexes is shown in Fig. 1. The coordination environment of the central Sb atom in **I** and **II** is intermediate between trigonal-bipyramidal and tetragonal-pyramidal ones. The parameter $\tau$ is 0.50 for both complexes [27]. The carboxylate groups in **I** and **II** occupy *cis*-positions. The key Sb(1)–O(1, 3), Sb(1)–O(2, 4), and Sb(1)–C(Ph) distances in **I** and **II** are in the 2.1196(3)–2.1512(8), 2.7778(9)–2.9816(4), 2.1063(4)–2.1190(3) Å ranges, respectively. According to CCDC data [28], these bond lengths are typical of triphenylantimony(V) carboxylate complexes. Note that the monoclinic (**I**) to triclinic (**II**) transition gives rise to two conformers, because of the disorder of one allyl moiety of the carboxylate ligand in **II** with occupan-

**Table 2.** Distances and key topological parameters for the CP(3, −1)* in the antimony coordination sphere of the $Ph_3Sb(O_2CCH_2{-}CH{=}CH_2)_2$ complex as the monoclinic and triclinic phases

| Bond | Distance, Å | ν(**r**), a.u. | ρ(**r**), a.u. | $\nabla^2\rho(\mathbf{r})$, a.u. | $h_e(\mathbf{r})$, a.u. |
|---|---|---|---|---|---|
| Monoclinic phase (**I**) | | | | | |
| Sb(1)−O(1) | 2.1255(9) | −0.102 | 0.077 | 0.272 | −0.017 |
| Sb(1)−O(3) | 2.1512(8) | −0.092 | 0.071 | 0.257 | −0.014 |
| Sb(1)···O(2) | 2.8384(10) | −0.017 | 0.024 | 0.068 | 0.0001 |
| Sb(1)···O(4) | 2.7778(9) | | | | |
| Sb(1)−C(9) | 2.1166(11) | −0.205 | 0.137 | −0.040 | −0.108 |
| Sb(1)−C(15) | 2.1102(12) | −0.166 | 0.117 | 0.063 | −0.075 |
| Sb(1)−C(21) | 2.1081(12) | −0.191 | 0.128 | 0.055 | −0.089 |
| Triclinic phase (**II**) | | | | | |
| Sb(1)−O(1) | 2.1196(3) | −0.138 | 0.099 | 0.198 | −0.044 |
| Sb(1)−O(3) | 2.1277(3) | −0.128 | 0.094 | 0.205 | −0.039 |
| Sb(1)···O(2) | 2.8021(4) | | | | |
| Sb(1)···O(4) | 2.9816(4) | | | | |
| Sb(1)−C(9) | 2.1190(3) | −0.147 | 0.105 | 0.161 | −0.053 |
| Sb(1)−C(15) | 2.1089(3) | −0.161 | 0.113 | 0.116 | −0.066 |
| Sb(1)−C(21) | 2.1063(4) | −0.174 | 0.121 | 0.058 | −0.080 |

* CP(3, −1) is the (3, −1) critical point.

cies of 80% (**IIa**) and 20% (**IIb**) (Fig. 1b). The disordered groups in triclinic phase **II** are roughly related by a mirror plane passing through the O(3)O(4)C(5) carboxylate group. Superposition of the $Ph_3Sb(O_2CCH_2{-}CH{=}CH_2)_2$ complex molecules for monoclinic (**I**) and triclinic (**IIa**, **IIb**) phases is shown in Fig. 2. The most pronounced conformational differences are between the C(6)C(7)C(8) moieties of the monoclinic (**I**) and triclinic (**IIa**) phases (Fig. 2a) and the C(6)C(7)C(8) and C(6')C(7')C(8') moieties of **I** and **IIb** (Fig. 2b). The C(6)C(7)C(8) allyl group of the vinylacetic ligand (80% site occupancy) of **IIa** is rotated through ~170° relative to the similar C(6)C(7)C(8) group of **I** around the $C_2$ axis extended along the C(5)–C(6) bond (Fig. 2a). In turn, the C(6')C(7')C(8') moiety of the vinylacetic ligand (20% site occupancy) of **IIb** and the C(6)C(7)C(8) moiety of **I** are roughly related by a mirror plane. Thus, the spontaneous transition of the monoclinic crystals **I** gives rise to two conformational isomers in the triclinic phase.

For studying the nature of chemical bonds in the Sb coordination sphere of **I** and **II**, we used Bader's theory [29], according to which the Sb(1)−O(1, 3) and Sb(1)−C(15, 21) bonds in **I** refer to the intermediate type of interactions ($\nabla^2\rho(\mathbf{r}) > 0$, $h_e(\mathbf{r}) < 0$), whereas the Sb(1)−C(9) bond is a shared interaction ($\nabla^2\rho(\mathbf{r}) < 0$, $h_e(\mathbf{r}) < 0$) (Table 2). In **II**, all interactions in the antimony coordination sphere are of intermediate type. Note that the Sb−C(Ph) bonds in the previously studied triphenylantimony dicarboxylate complexes were characterized as either intermediate [30, 31] or shared type interactions [32].

To reveal the nature of conformational polymorphism in the $Ph_3Sb(O_2CCH_2{-}CH{=}CH_2)_2$ crystals, all interactions between the complex molecules in the monoclinic (**I**) and triclinic (**II**) phases were identified and their energies were estimated using the Espinosa–Molins–Lecomte correlation [33]. It is of interest that the energy of intermolecular contacts of the O(1, 2)C(1−4) ligand in the monoclinic polymorph **I** (−9.41 kcal/mol) virtually coincides with the corresponding energy value for this ligand in the triclinic polymorph **II** (−9.49 kcal/mol). This is in line with the moderate conformational changes of the O(1.2)C(1−4) ligand upon conversion to the triclinic phase **II**. Meanwhile, the O(3, 4)C(5−8) ligand undergoes much more pronounced conformational changes upon the monoclinic (**I**) to triclinic (**II**) transition. The energy of intermolecular contacts of this ligand in **I** is −8.01 kcal/mol, which is smaller than that in **IIa** (−10.25 kcal/mol) or **IIb** (−8.42 kcal/mol). As a result of phase transition, the crystal lattice energy decreases by ~5 kcal/mol in **IIa** and ~3.5 kcal/mol in **IIb**; also, the molecular volumes decrease and, hence, the density and the packing factor increase (Table 3). It is noteworthy that the volume of the C(6)C(7)C(8) allyl group in **I**, including hydrogen atoms, found as the sum of atomic basins is 76.3 Å$^3$, which is markedly greater than the volume of analogous group in **II** (73.9 Å$^3$ in **IIa** and 72.9 Å$^3$ in **IIb**). This difference can be interpreted as being due to the presence of voids around the C(6)C(7)C(8) allyl group in **I**, which

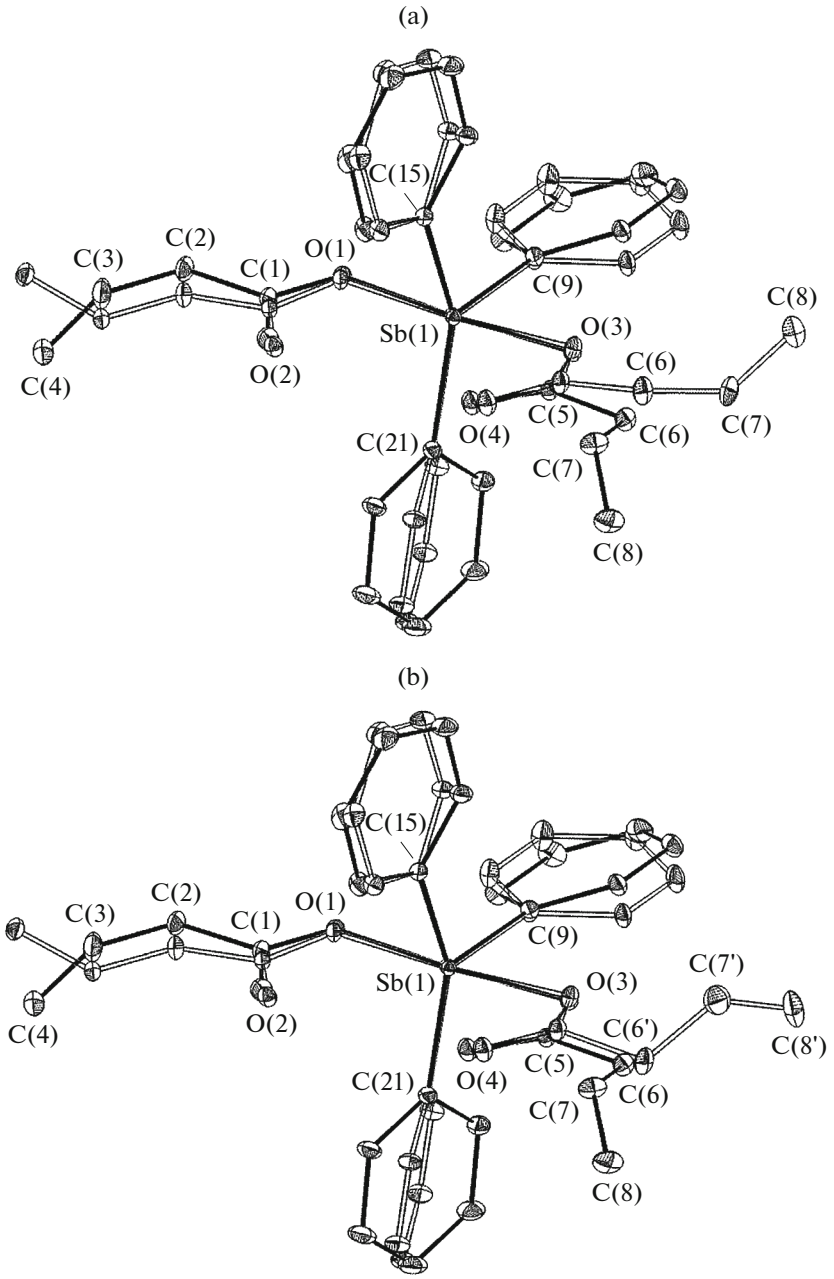


**Fig. 2.** Superposition of molecules of $Ph_3Sb(O_2CCH_2{-}CH{=}CH_2)_2$ in monoclinic (**I**) and triclinic ((a) **IIa** and (b) **IIb**) phases. The bonds are shown by solid lines in the monoclinic phase molecules and by contour lines in triclinic phase molecules. The thermal ellipsoids are drawn at the 30% probability level. Hydrogen atoms are omitted for clarity.

allows this group to change conformation without crystal destruction (Fig. 3).

Thus, the presence of voids near one of the carboxylate ligands in the monoclinic phase (**I**) of $Ph_3Sb(O_2CCH_2{-}CH{=}CH_2)_2$ decreases the energy of intermolecular interactions and, hence, enables a conformational change with a pronounced decrease in the crystal lattice energy. In other words, the voids present in the crystals of monoclinic phase **I** provide a way to thermodynamically more favorable molecular conformation in the crystal.

## ACKNOWLEDGMENTS

This work was performed using the scientific equipment of the Center for Collective use "Analytical Center of the Institute of Organometallic Chemistry, Russian Academy of Sciences."

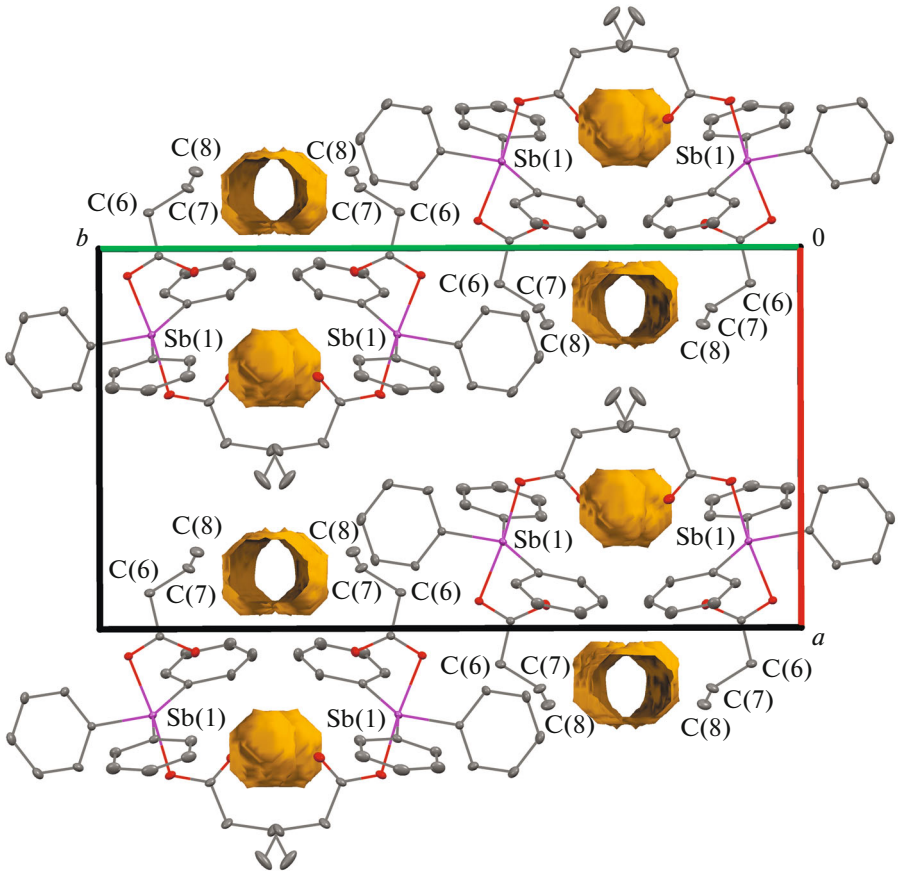


**Fig. 3.** Positions of voids in the monoclinic phase (**I**) of the $Ph_3Sb(O_2CCH_2{-}CH{=}CH_2)_2$ complex.

**Table 3.** Energy and crystal characteristics of the $Ph_3Sb(O_2CCH_2{-}CH{=}CH_2)_2$ complex

| Monoclinic phase (**I**) | Triclinic phase (**II**)* |
|---|---|
| Energy of all intermolecular contacts, kcal/mol | |
| –40.04 | –45.72/–43.50 |
| Density, g/cm$^3$ | |
| 1.486 | 1.554 |
| Packing factor, % | |
| 70.2 | 73.3/73.1 |
| Volume of the molecule (sum of the Voronoi–Dirichlet polyhedra), Å$^3$ | |
| 596.2 | 565.5 |
| Volume of the molecule (sum of the atomic basin volumes), Å$^3$ | |
| 582.8 | 557.3 |

* The values for **IIb** are given after the slash.


## FUNDING

This work was supported by the Russian Foundation for Basic Research (project no. 17-03-01257).


## REFERENCES


1. Bajpai, K., Singhal, R., and Srivastava, R.C., *Indian J. Chem., Sect. A: Inorg., Bio-Inorg., Phys., Theor. Anal. Chem.*, 1979, vol. 18, p. 73.
2. Singhal, K., Rastogi, R., and Raj, P., *Indian J. Chem., Sect. A: Inorg., Bio-Inorg., Phys., Theor. Anal. Chem.*, 1987, vol. 26, p. 146.
3. Ma, Y., Li, J., Xuan, Z., and Liu, R., *J. Organomet. Chem.*, 2001, vol. 620, nos. 1–2, p. 235.
4. Liu, R.-C., Ma, Y.-Q., Yu, L., et al., *Appl. Organomet. Chem.*, 2003, vol. 17, no. 9, p. 662.
5. Yu, L., Ma, Y.-Q., Liu, R.-C., et al., *Polyhedron*, 2004, vol. 23, no. 5, p. 823.
6. Yu, L., Ma, Y.-Q., Wang, G.-C., et al., *Heteroat. Chem.*, 2004, vol. 15, no. 1, p. 32.
7. Hadjikakou, S.K., Ozturk, I.I., Banti, C.N., et al., *J. Inorg. Biochem.*, 2015, vol. 153, p. 293.
8. Islam, A., Rodrigues, B.L., Marzano, I.M., et al., *Eur. J. Med. Chem.*, 2016, vol. 109, p. 254.
9. US Patent 3287210, 1966.

10. *Organometallic Polymers*, Carraher, C.E., Pittman, C.U., and Sheats, J.E., Eds., Elsevier, 1978.
11. Koton, M.M.: *Metalloorganicheskie soedineniya i radikaly* (Organometallic Compounds and Radicals), Moscow: Nauka, 1985.
12. Gushchin, A.V., Moiseev, D.V., and Dodonov, V.A., *Russ. Chem. Bull.*, 2001, vol. 50, no. 7, p. 1291.
13. Moiseev, D.V., Gushchin, A.V., Shavirin, A.S., et al., *J. Organomet. Chem.*, 2003, vol. 667, nos. 1–2, p. 176.
14. Qin, W., Yasuike, S., Kakusawa, N., et al., *J. Organomet. Chem.*, 2008, vol. 693, no. 17, p. 2949.
15. Passarelli, J., Murphy, M., Del Re.R., et al., *SPIE Advanced Lithography*, 2015, vol. 9425, p. 94250.
16. Gushchin, A.V., Sharutin, D.V., Prytkova, L.K., et al., *Zh. Obshch. Khim.*, 2011, vol. 81, no. 3, p. 493.
17. *Data Collection. Reduction and Correction Program*, CrysAlis Pro-Software Package, Agilent Technologies, 2012.
18. *SAINT. Data Reduction and Correction Program, Version 8.27B*, Madison: Bruker AXS Inc., 2012.
19. *SCALE3 ABSPACK: Empirical Absorption Correction. CrysAlis Pro-Software Package*, Agilent Technologies, 2012.
20. Sheldrick, G.M., *SADABS-2012/1. Bruker/Siemens Area Detector Absorption Correction Program*, Madison (WI, USA): Bruker AXS Inc., 2012.
21. Sheldrick, G.M. *SHELXTL. V.6.14. Structure Determination Software Suite*, Madison: Bruker AXS, 2003.
22. Hansen, N.K. and Coppens, P., *Acta Crystallogr., Sect. A: Cryst. Phys., Diffr., Theor. Gen. Crystallogr.*, 1978, vol. 34, no. 6, p. 909.
23. Jelsch, C., Guillot, B., Lagoutte, A., et al., *J. Appl. Crystallogr.*, 2005, vol. 38, no. 1, p. 38.
24. Allen, F.H., Kennard, O., Watson, D.G., et al., *J. Chem. Soc., Perkin Trans.*, 1987, no. 12, p. 2.
25. Hirshfeld, F., *Acta Crystallogr., Sect. A: Cryst. Phys., Diffr., Theor. Gen. Crystallogr.*, 1976, vol. 32, no. 2, p. 239.
26. Stash, A. and Tsirelson, V., *J. Appl. Crystallogr.*, 2002, vol. 35, no. 3, p. 371.
27. Addison, A.W., Rao, T.N., Reedijk, J., et al., *Dalton Trans.*, 1984, no. 7, p. 1349.
28. Groom, C.R., Bruno, I.J., Lightfoot, M.P., et al., *Acta Crystallogr.*, 2016, vol. 72, no. 2, p. 171.
29. Bader, R.F.W., *Atoms in Molecules, A Quantum Theory*, Oxford: Oxford Univ. Press, 1990.
30. Fukin, G.K., Samsonov, M.A., Kalistratova, O.S., et al., *Struct. Chem.*, 2016, vol. 27, no. 1, p. 357.
31. Fukin, G.K., Samsonov, M.A., Arapova, A.V., et al., *J. Solid State Chem.*, 2017, vol. 254, p. 32.
32. Fukin, G.K., Samsonov, M.A., Baranov, E.V., et al., *Russ. J. Coord. Chem.*, 2018, vol. 44, no. 10, p. 626. https://doi.org/10.1134/S1070328418100020
33. Espinosa, E., Molins, E., and Lecomte, C., *Chem. Phys. Lett.*, 1998, vol. 285, nos. 3–4, p. 170.

*Translated by Z. Svitanko*